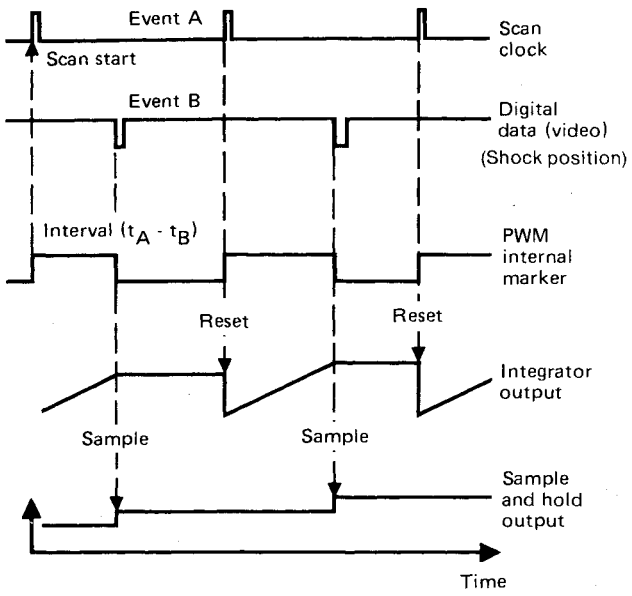

Fig. 3 Timing and control of decoding circuit.

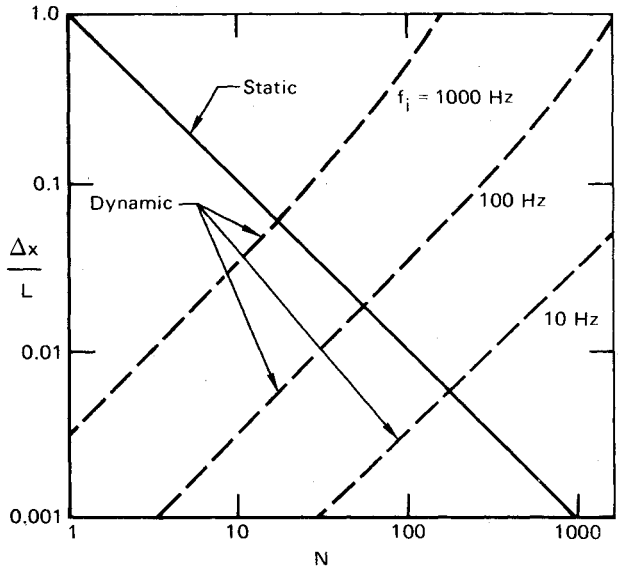

Fig. 4 Static and dynamic errors for an image moving sinusoidally with amplitude $A = L/2$ and frequency f_i.

rods of 1.6-mm diam were placed at known streamwise locations into the field of view, the voltage outputs were manually recorded; and the constants A and B were determined by a least-square fit. The calibrations were executed before and after each run.

System Accuracy

The spatial resolution for a stationary object (Δx_s) is determined primarily by the pixel spacing. The resolution in the image plane is

$$\Delta x_s/L = 1/N \tag{2}$$

where L is the array length (6.35 mm in this case).

If the object is moving, each indicated light-intensity distribution shows a blur whose width is equal to the distance traveled by the shock image between two successive scans. If the image is a sharp, black-to-white boundary moving at a constant speed u, the indicated light-intensity distribution shows a linear variation from low to high level over a distance Δx_b. This distance represents the upper limit of the dynamic error and is given by

$$\frac{\Delta x_b}{L} \leq \frac{N}{(f_s L/u) - N} \tag{3}$$

If the trigger level is set halfway between the high and low levels, the system will yield, in principle, image positions with zero dynamic error. Other trigger levels will result in speed-dependent errors, all less than Δx_b. If the image oscillates sinusoidally with amplitude A and frequency f_i, the maximum blur distance can be estimated using Eq. (3), with $u = 2\pi f_i A$, provided $f_i \ll f_f$. Figure 4 illustrates both types of errors.

The requirements of small static and dynamic uncertainties are conflicting: high spatial resolution means greater blur distance for a given image speed, provided the scan rate f_s (pixels/s) is fixed. Since sensor arrays are available with various pixel numbers, N can be chosen during design for an acceptable compromise. Both errors are referred to the image size; errors in the actual flow are proportional to the ratio of the corresponding linear dimensions of object and the image, as controlled by the optics of the shadowgraph system.

The optical system must be of high quality. Density striations in the test-section walls of commercial mirror glass (used in the first series of tests) introduced light-level variations in the shock-free background that were significant compared to variations typical of shock signatures. Room thermals and a slight drift in camera clock frequency were secondary error sources.

The preceding problems were resolved without undue effort. We consider the system as a viable option for determining the displacement history of any low-speed, visible motion. The method could also be useful in low-speed experiments involving dye- or smoke-visualized, unsteady flows, since the edges of boundary or free shear layers could be detected. The cost of the apparatus is significantly less than that of a general-purpose, two-dimensional image processing system.

Acknowledgment

This research was conducted under the McDonnell Douglas Independent Research and Development Program.

Reference

[1] Chen, C.P., Sajben, M., and Kroutil, J.C., "Shock Wave Oscillations in a Transonic Diffuser Flow," *AIAA Journal* (scheduled for publication in the Sept. 1979 issue).

Rayleigh Scattering Measurements of Time-Resolved Concentration in a Turbulent Propane Jet

T. Michal Dyer*
Sandia Laboratories, Livermore, Calif.

A METHOD has been developed whereby laser Rayleigh scattering is used to determine time- and space-resolved fuel/air concentrations in propane air mixtures. The technique was statically calibrated using prepared homogeneous mixtures in a closed vessel, then was applied to concentration fluctuation measurements in a turbulent,

Received Feb. 20, 1979.

Index categories: Combustion and Combustor Designs; Jets, Wakes and Viscid-Inviscid Flow Interactions; Research Facilities and Instrumentation.

*Member Technical Staff, Combustion Applications Division.

axisymmetric propane jet. The advantages of this technique are its simplicity, ease of implementation, and the fact that it provides a real-time, spatially resolved measurement of propane mole fraction.

The fundamental principle governing laser Rayleigh scattering is that elastic collisions between gas molecules and an incident laser beam scatter that light at the laser wavelength. The intensity of the scattered light, in general, is directly proportional to the laser power, the gas density, and a cross section dependent on the gas that is being investigated. For a multicomponent gas such as fuel vapor/air mixture, the contributions to the total signal are independent for each gas and depend only on each component's partial pressure (density) and cross section; thus

$$I \propto (P_T/T)\,(f_F\sigma_F + f_A\sigma_A) \qquad (1)$$

where I is the Rayleigh scattered signal, P_T and T are total mixture pressure and temperature, f_F and f_A are fuel and air mole fractions, and σ_F and σ_A are the appropriate Rayleigh scattering cross sections. Thus, if the cross sections, pressure, and temperature are known, f_F/f_A may be determined from the Rayleigh signal level. The fundamental criterion which allows this technique to work is that the fuel and air must have greatly different cross sections. For example, σ_F for propane is about 13.5 times σ_A for air; therefore small changes in propane mole fraction result in large changes in signal levels.

The technique has been calibrated using quiescent homogeneous mixtures in a closed vessel shown schematically in Fig. 1. An argon-ion laser beam (nominally 1.5 W at 4880 Å) is propagated diametrically across the chamber and dumped on the opposite side. A narrow slice (0.125 mm) of the scattered light is collected and its intensity measured with a photomultiplier tube (PMT) (Hamamatsu R928). A 10-Å narrow bandpass filter is employed to reject extraneous light. The magnification of the f2.5 optical system is unity, and proper focus is checked by traversing a 0.1-mm wire illuminated by the laser. The time-resolved PMT signal is recorded and analyzed on an on-line PDP 11/34 minicomputer. The resulting steady-state calibration curves are shown in Fig. 2. The plot shows PMT signal vs total mixture pressure with propane mole fraction as a parameter. The large separation of the curves indicate good signal sensitivity to changes in concentration. The lines which appear to connect the data points are derived from Eq. (1), taking into proper account background scattered light. The ratio σ_F/σ_A is determined experimentally to be 13.50 for 99.5% pure C_3H_8.

In order to exploit the advantages of Rayleigh scattering, measurements were taken of the turbulent concentration fluctuations in an axisymmetric propane jet. Such measurements have been acquired in the past using smoke scattering,[1] pulsed Raman scattering,[2] and Ramam photon correlation techniques.[3] The recent work by Birch et al.[3]

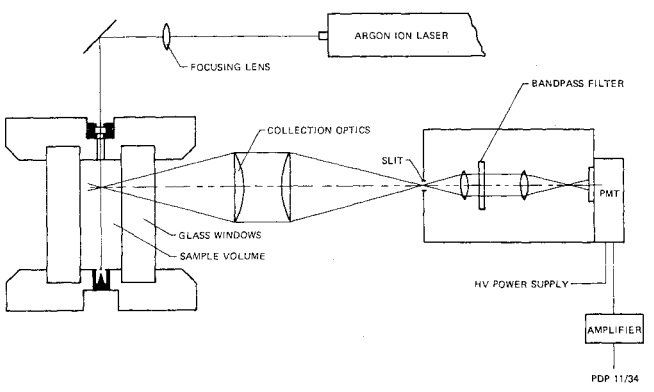

Fig. 1 Schematic outline of Rayleigh scattering experimental apparatus: temporal and spatial fuel concentration.

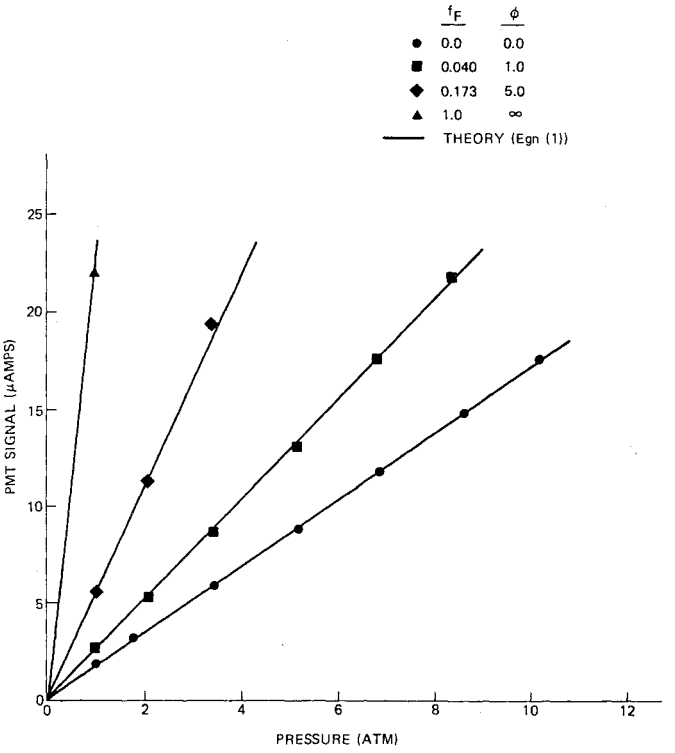

Fig. 2 Static calibration of Rayleigh-scattered signal vs pressure for various propane/air mixtures. Concentration is shown as f_F, propane mole fraction, and ϕ, fuel/air equivalence ratio. Temperature is held fixed at 300 K. Data compare favorably with analytical model [Eq. (1)].

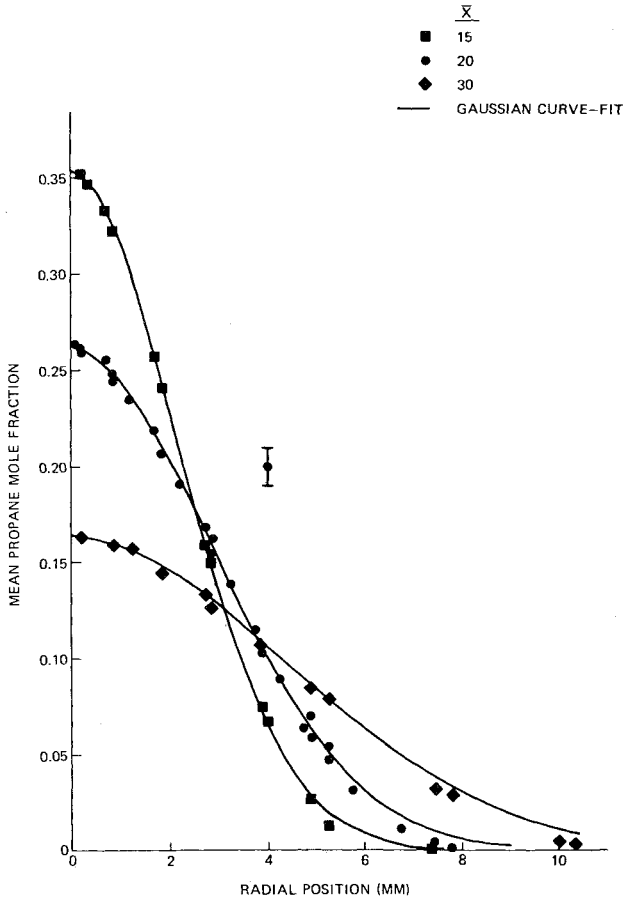

Fig. 3 Radial profiles of mean propane mole fraction at various axial positions above the jet tip. Data are compared to a universal Gaussian curve fit.

using photon correlation perhaps represents a breakthrough in analyzing the inherently low Raman signal levels to obtain meaningful concentration fluctuation profiles in the round jet. The Rayleigh technique described here is proposed as a more straightforward approach to the same problem.

The experimental apparatus is the same as shown in Fig. 1 except that the pressure vessel is replaced by the free jet. The laser is focused along a line normal to the jet centerline, and Rayleigh scattered light is collected again at right angles to the beam. The laser beam diameter is approximately 200 μ, which defines the spatial resolution of the optical system. The laser and collection optics are all mounted on a milling machine table which allows repeatable three-dimensional scanning to better than 0.05 mm.

The propane jet is a 2.0-mm-diam tube 20-mm long tapered along the outside to a narrow lip at the jet exit. The jet is surrounded by a coaxial air flow of velocity 0.7 m/s provided from a bottled source. This step was taken to provide a dust-free environment, since particles produce problems because of their large Mie scattering at the same wavelength as the Rayleigh signal. The propane jet velocity was 21.1 m/s and the jet Reynolds number based on the exit diameter was 9790.

For the special case of a uniform pressure, isothermal experiment, Eq. (1) reduces to a simpler form:

$$f_F = \frac{(I/I_0) - 1}{12.5}$$

where I is the measured signal after the subtraction of background scattered light and I_0 is the air-only value of signal minus background. Therefore, a simple ratio of the measured instantaneous signal to the air-only signal far from the jet centerline provides the desired time-resolved value of propane mole fraction. Careful optical design allows the background scattered light to be reduced to about 1% of the air-only signal.

Radial profiles of mean propane concentration are shown in Fig. 3 for three axial positions of $\bar{x} = 15$, 20, and 30, where $\bar{x}$ is the axial position normalized by the jet diameter. These data may be readily collapsed to a single curve by normalizing the propane mole fraction by its centerline value and normalizing the radial coordinate r by $r_{1/2}$, the position where the concentration has dropped to one-half the centerline value. To support this statement the data for each profile have been compared on the figure with universal Gaussian curves having the form:

$$\frac{f_F}{f_{F_\ell}} = \exp\left[-0.6931\left(\frac{r}{r_{1/2}}\right)^2\right]$$

This fact, in concert with the fact that $r_{1/2}/x$ is a constant ($=0.0855$) to within 1% for all three profiles, indicates that the jet is closely approaching its self-preserving state. These normalized profiles are in close agreement with the data Birch et al.[3] in a turbulent methane jet except that the spreading rate is slightly less with propane. Such a density dependence on spread rate is consistent with the trends established using data on air jets by Becker et al.[1] and the theoretical analysis of Kleinstein.[4]

The rms standard deviation of the concentration fluctuations along a radial profile at $\bar{x} = 20$ is plotted in Fig. 4. The rms concentration fluctuation normalized by the local mean value is 18% on the axis and increases monotonically with r. The absolute fluctuation intensities reach a maximum value of 19% above the centerline value at a normalized radius near 0.7, consistent with the results of Birch et al.[3]

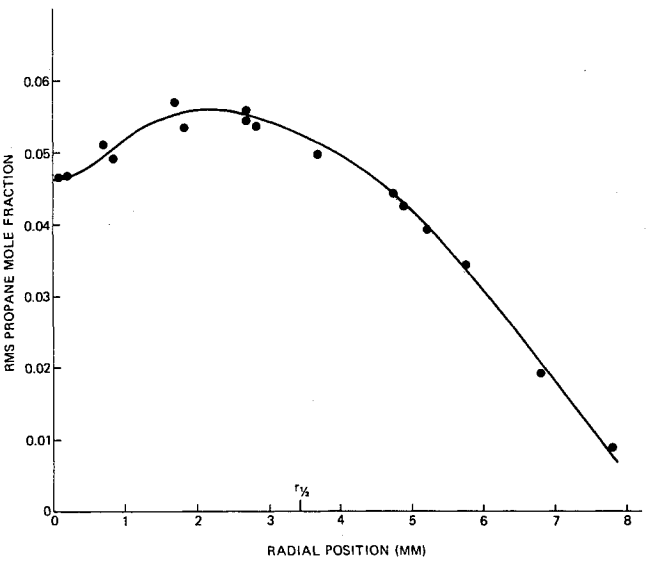

Fig. 4 Radial profile of rms propane mole fraction fluctuation at the axial position, $x/d = \bar{x} = 20$.

The autocorrelation of the data record has also been performed to gain some insight into the time and length scales associated with turbulent free jets. The autocorrelation function has been fitted with an exponential decay whose e-folding time delay is the Eulerian integral time scale. The integral time scale on the centerline is approximately 140 μs, increasing with r as expected to approximately 315 μs at the $r/r_{1/2}$ position. These data may be combined with the empirical centerline velocity decay correlations of Witze[5] for ideal turbulent free jets to arrive at an estimate for the integral length scale. The approximate centerline velocity is calculated to be 800 cm/s, which yields an integral length scale at $\bar{x} = 20$ of 1.12 mm.

An error analysis has been performed to account for statistical biasing due to PMT noise and standard errors due to the finite record length for the data analysis. The result is that because of the relatively long data record (7500 points at 30-μs intervals), statistical standard errors are small. The bias in the rms standard deviation as a result of PMT noise lies within the system error bars due to jet unsteadiness and experimental repeatability. Mean and rms propane mole fractions are conservatively estimated to be accurate to within 0.01.

Acknowledgment

The author would like to acknowledge many helpful discussions and reviews by P. O. Witze and R. W. Dibble, and computer programming assistance by J. E. Fertig. This work was funded by the Division of Fossil Fuel Utilization of the Department of Energy and the Motor Vehicle Manufacturers Association.

References

[1] Becker, H. A., Hottel, H. C., and Williams, G. C., "The Nozzle Fluid Concentration Field of the Round Turbulent Free Jet," *Journal of Fluid Mechanics*, Vol. 30, Nov. 1967, pp. 285-303.

[2] Widhopf, G. F. and Lederman, S., "Species Concentration Measurements Utilizing Raman Scattering of a Laser Beam," *AIAA Journal*, Vol. 9, Feb. 1971, pp. 309-316.

[3] Birch, A. D., Brown, D. R., Dobson, M. G., and Thomas, J. R., "The Turbulent Concentration Field of a Methane Jet," *Journal of Fluid Mechanics*, Vol. 88, Oct. 1978, pp. 431-449.

[4] Kleinstein, G., "Mixing in Turbulent Axially Symmetric Free Jets," *Journal of Spacecraft and Rockets*, Vol. 1, July-Aug. 1964, pp. 403-408.

[5] Witze, P. O., "Centerline Velocity Decay of Compressible Free Jets," *AIAA Journal*, Vol. 12, April 1974, pp. 417-418.